Competition between single-particle and collective excitations in $N=88$ nuclei: Measurement of $g(4_1^+)/g(2_1^+)$ in ^{152}Gd

N. A. Matt,[1,*] N. Benczer-Koller,[1] J. Holden,[1] G. Kumbartzki,[1] R. H. Mayer,[1,†] M. Satteson,[1,‡] and R. Tanczyn[2,§]
[1]*Department of Physics and Astronomy, Rutgers University, New Brunswick, New Jersey 08903*
[2]*Department of Physical Sciences, Kutztown University, Kutztown, Pennsylvania 19530*
(Received 23 September 1998)

The magnetic moment of the 2_1^+ and 4_1^+ states in ^{152}Gd have been measured by the transient field technique. Heavy ion beams of ^{58}Ni and ^{32}S were used to Coulomb excite the 2_1^+, 0_2^+, 4_1^+, 2_2^+, and 6_1^+ states in ^{152}Gd. A ratio of g factors, $g(4_1^+)/g(2_1^+)=1.10(24)$ was obtained. This result is consistent with a collective model description and does not support large single particle contributions to the wave function of low-lying states as were found for the isotone ^{150}Sm. [S0556-2813(99)05302-9]

PACS number(s): 21.10.Ky, 27.70.+q

I. INTRODUCTION

Magnetic moments of nuclear states provide stringent tests for nuclear models, and are particularly sensitive to the interplay of single particle degrees of freedom with the collective excitations of the core. In particular, a recent g factor measurement in ^{150}Sm has yielded a ratio of g factors, $g(4_1^+)/g(2_1^+)=1.60(12)$, much larger than expected on the basis of a pure collective description [1] and in disagreement with an earlier measurement that yielded $g(4_1^+)/g(2_1^+)=0.85(11)$ [2]. Medium-weight nuclei far from closed shells are best described by collective models. However, in the IBA-II model, both ^{152}Gd and ^{150}Sm have proton numbers close to the subshell at $Z=64$. The subshell gap at $Z=64$ disappears for $N\geqslant 88$ as neutrons filling the $h_{11/2}$ orbital interact with the protons in the $h_{9/2}$ orbital and contribute to promotions of protons across the gap. The anomalously high value of the g factor ratio observed in ^{150}Sm signals a change in the structure of the state as a function of spin and can be interpreted as an indication that the number of protons contributing to the collective motion is larger for the 4_1^+ state than for the 2_1^+ state. In particular, the g factors of other yrast states in neighboring nuclei with $N\sim 88$ and $Z\sim 60-66$ could be used as a measure of changes in the effective number of valence protons with increasing angular momentum and as a check of whether the disappearance of the $Z=64$ subshell gap is sharper at higher excitation energies and spins. A study of the systematics of the 4_1^+ moments in this region, therefore, may elucidate any structural changes that occur with increasing angular momentum.

The magnetic moment of the 2_1^+ state had previously been determined by the recoil into gas and vacuum method, $g(2_1^+)=0.48(4)$ [3] and by the transient field technique, $g=0.45(4)$ [4]. However, the g factor of higher spin states have not been determined. In the present measurement, the 4_1^+, 0_2^+, 2_2^+, and 6_1^+ states were excited, but only the 2_1^+ and 4_1^+ states were populated with sufficient intensity to allow a magnetic moment measurement.

II. EXPERIMENTAL PROCEDURES

In the conventional application of the transient field technique target nuclei are excited by heavy ion beams and are simultaneously ejected from the target material with high velocity. These fast ions subsequently traverse a ferromagnetic material such as iron or gadolinium in which they interact with the polarized electrons. This interaction yields an effective hyperfine field at the nucleus which results in a precession of the angular distribution of decay γ rays. This angular precession is directly proportional to the magnetic moment of the excited state under study. The experimental details for measuring magnetic moments of short-lived excited states by the transient field technique have been described in detail in previous publications [5,6]. Only the details relevant to the current experiments are elaborated upon here.

In the present experiment, ^{152}Gd ions were Coulomb excited by ^{58}Ni and ^{32}S beams at Yale University's Wright Nuclear Structure Laboratory. The states of interest in ^{152}Gd were populated through Coulomb excitation by beams of ^{58}Ni at 180, and 212.5 MeV, as well as ^{32}S ions at 100 MeV. Figure 1 displays the low-energy levels of ^{152}Gd.

The targets consisted of Gd (enriched to 20% in ^{152}Gd for runs I and II and 40% for run III), evaporated onto iron foils. The iron foil thickness was chosen to ensure that the recoiling Gd nuclei exited from the ferromagnetic foil with a velocity $\geqslant 2v_0$ where v_0 is the Bohr velocity. The iron foils were annealed in a hydrogen atmosphere for four hours at 900 °C. The magnetization of the iron foil was measured in an ac magnetometer [7] before and after each experiment to an accuracy of 5%. The specifics of the target compositions and of the kinematics of the reactions for the three runs are presented in Tables I and II. During the experiment the targets were polarized by a magnetic field of 0.03 T, sufficient to saturate the iron foil. The field direction was reversed in four minute intervals throughout the precession measurements. Four Ge detectors (of approximately 25% efficiency)

*Present address: Microsoft Corporation, Redmond, WA 98052-6399.

†Present address: School of Chemical Engineering, Purdue University, West Lafayette, IN 47907.

‡Present address: Interventional Innovations, 2670 Patton Road, St. Paul, MN 55113.

§Deceased.

 ©1999 The American Physical Society

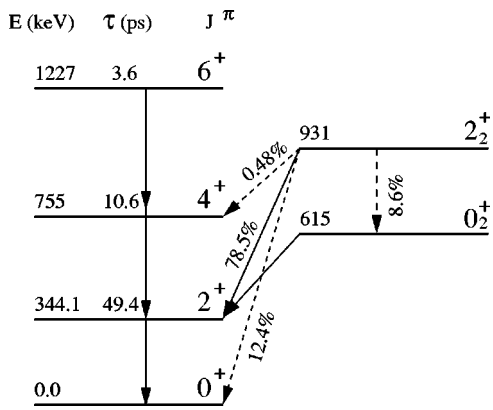

FIG. 1. Energy level diagram of the low-lying levels in ^{152}Gd.

detected the γ rays in coincidence with backscattered beam ions in an annular silicon surface-barrier detector subtending an angle between 166° and 177°. This coincidence requirement ensures that the observed decays originate in states with large initial alignment, and that the momentum transfer to the recoiling ^{152}Gd ions was large enough for the ions to traverse the ferromagnet and come to rest in the copper backing of the target. The Ge detectors were positioned at $\pm 64°$ and $\pm 116°$ with respect to the beam axis in order to provide maximum sensitivity for the precession measurement. The recoil beam particle energy, the γ-ray energy as well as the time interval between particle and γ-ray energy signals were recorded for each event. A typical γ-ray spectrum is shown in Fig. 2.

A typical angular distribution is displayed in Fig. 3.

III. DATA ANALYSIS AND RESULTS

The traversal time through the ferromagnet is short ($\sim$0.7 ps) compared to the lifetimes of the excited states, hence the precession of the nuclear spin in the transient field occurs mainly in the state originally excited by the target-beam collision. In the present experiment, several excited states are simultaneoulsy excited. It is not possible to separate the γ rays which are emitted by a nucleus which is directly Coulomb excited from the γ rays emitted by nuclei in states that are populated in the decay of higher states. However, the precession of interest can be extracted from the average precession measured since the population of excited states is determined from Coulomb excitation calculations, and the γ-ray angular distribution of the subsequent γ-ray cascade is known.

In general, the measured precession effect ϵ^n for the radiation deexciting a state n can be expressed as $\epsilon^n = (\rho^n - 1)/(\rho^n + 1)$, where $\rho^n = (\rho^n_{14}/\rho^n_{23})$ is determined

TABLE I. Description of the composition of the multilayered targets.

Run	Gd (mg/cm^2)	Fe (mg/cm^2)	Cu (mg/cm^2)	M (T)
I	0.260	3.98	10.9	0.1707
II	0.390	4.82	6.6	0.1707
III	0.350	1.92	6.7	0.1511

TABLE II. Characteristics of the reaction kinematics. $\langle E_{\rm in}\rangle$, $\langle E_{\rm out}\rangle$, $\langle v_{\rm in}/v_0\rangle$, and $\langle v_{\rm out}/v_0\rangle$ are, respectively, the average energies and velocities of the ^{152}Gd ions as they enter into and exit from the gadolinium foil. $v_0 = e^2/\hbar$ is the Bohr velocity.

Run	Beam	Beam energy (MeV)	$\langle E_{\rm in}\rangle$ (MeV)	$\langle E_{\rm out}\rangle$ (MeV)	$\left\langle \frac{v_{\rm in}}{v_0}\right\rangle$	$\left\langle \frac{v_{\rm out}}{v_0}\right\rangle$
I	^{58}Ni	180	138.5	22.7	6.1	2.4
II	^{58}Ni	212.5	161.5	18.1	6.5	2.2
III	^{32}S	100	53.9	17.4	3.8	2.2

from the double ratios $\rho^n_{ij} = \sqrt{(N_i^{\uparrow n}/N_i^{\downarrow n})/(N_j^{\uparrow n}/N_j^{\downarrow n})}$, and the coefficients $i=1,2$, $j=3,4$ represent the four detectors; $N^{\uparrow n}_{i,j}$ and $N^{\downarrow n}_{i,j}$ are the coincidence counting rates of the photopeak of the transition $I_n \rightarrow I_{n-1}$ in the ith or jth detector with the external field pointing ''up'' ($\uparrow$) or ''down'' ($\downarrow$) with respect to the plane of the reaction. The γ-ray photopeak intensities have been corrected for random and background rates. Similar ''cross ratios'' $\rho^n_c = (\rho^n_{24}/\rho^n_{13})$ and ϵ^n_c were calculated to check for systematic effects that might mask the true precession. In all cases, vanishingly small ϵ^n_c were obtained. The precession angles $\Delta\theta$ are derived from the measured ϵ's through the relationship $\Delta\theta = \epsilon/S$ where S is the logarithmic slope $S(\theta_0) = (1/W)(dW/d\theta)$ of the angular correlation at the detector angles.

The determination of the precession angles $\Delta\theta$ of the 6^+_1, 2^+_2, and 4^+_1 states follows directly from the measured precession and the slope of the angular distribution. However, the determination of the precession angle $\Delta\theta$ for the 2^+_1 states required a more elaborate analysis due to significant contributions to the precession from feeding from the 0^+_2, 2^+_2, and the 4^+_1 precursor states. This feeding affects the precession in two ways: (i) the *slope* of the measured ($2^+_1 \rightarrow 0^+_1$) angular correlation is a composite of contributions from the feeding states, and (ii) the *precessions* of the 4^+_1

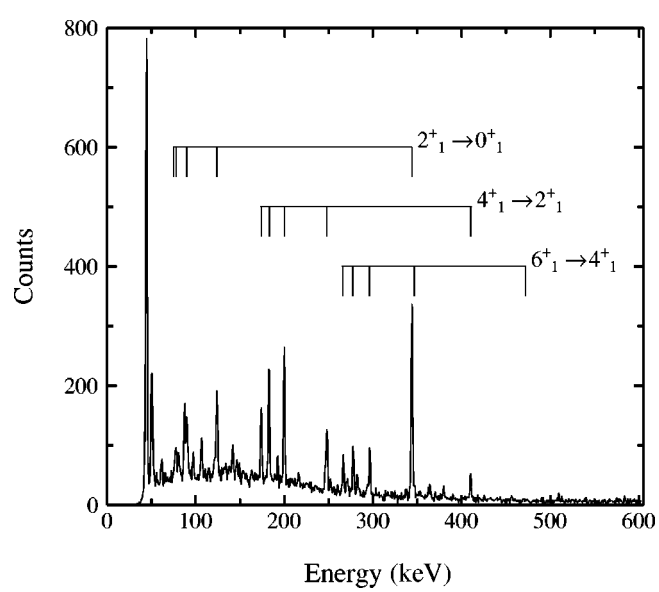

FIG. 2. γ-ray spectrum in ^{152}Gd in coincidence with backscattered beam of ^{58}Ni ions. The five vertical bars correspond sequentially, from left to right, to transitions in ^{160,158,156,154,152}Gd.

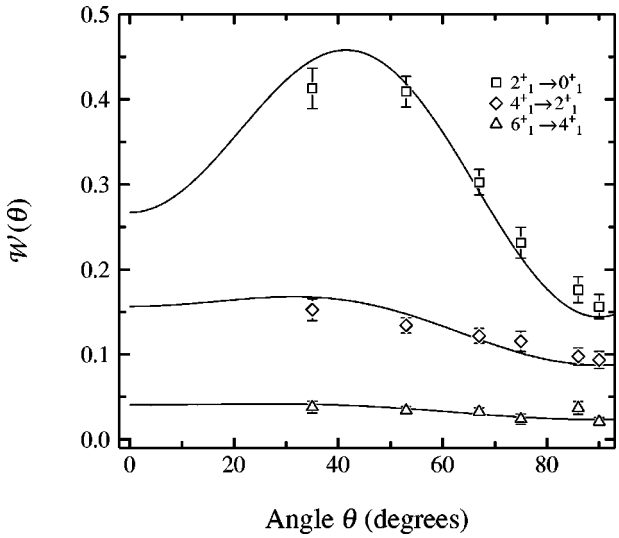

FIG. 3. Angular correlations observed for three transitions in ^{152}Gd.

and 2_2^+ states themselves (the 0_2^+ state does not precess) must be taken into account explicitly. Both these effects are characterized by the population strength of the feeding states and by the angular correlations in which the feeding transitions to the 2_1^+ state are not observed. The specific details of the analysis are discussed in Ref. [8].

An average measured effect $\langle \epsilon \rangle$ for the 2_1^+ state can be expressed as

$$\langle \epsilon \rangle = \epsilon_{2_1^+}^{\text{meas}} = \frac{\sum_i \epsilon_i P_i W_i(\theta_0)}{\sum_i P_i W_i(\theta_0)}, \tag{1}$$

where ϵ_i, P_i, and $W_i(\theta_o)$ represent the parameters of the states which are fed directly. W_i is the correlation function at θ_0 of the ith transition and P_i is the population strength of the feeding states proportional to the total Coulomb excitation cross section (Table III). Similarly, the average slope $\langle S \rangle$ which is directly related to the measured angular correlation can be expressed in terms of $S_i(\theta_o)$, the logarithmic slope of the angular correlation at θ_0 of the ith transition, as

$$S^{\text{meas}} \equiv \langle S \rangle = \frac{\sum_i S_i(\theta_0) P_i W_i(\theta_0)}{\sum_i P_i W_i(\theta_0)}. \tag{2}$$

TABLE III. Calculated Coulomb excitation level populations $P(I)$ for the 2_1^+, 0_2^+, 4_1^+, 2_2^+, and 6_1^+ states in ^{152}Gd at the indicated beam energies.

Run	Beam	Energy (MeV)	$P(2_1^+)$	$P(0_2^+)$	$P(4_1^+)$	$P(2_2^+)$	$P(6_1^+)$
I	^{58}Ni	180	0.571	0.165	0.182	0.049	0.034
II	^{58}Ni	212.5	0.356	0.195	0.224	0.136	0.089
III	^{32}S	100	0.737	0.105	0.131	0.014	0.013

TABLE IV. Summary of precessions and resulting g factors.

Run	$\Delta\theta(2_1^+)$	$\Delta\theta(4_1^+)$	$\Delta\theta(6_1^+)$
I	37.8(22)	38.2(115)	21.3(530)
II	31.0(48)	34.7(148)	24.0(221)
III	13.5(24)	16.3(65)	
Run	$g(2_1^+)$	$g(4_1^+)$	$g(6_1^+)$
I	0.460(27)	0.474(143)	0.278(691)
II	0.312(48)	0.357(152)	0.262(241)
III	0.321(57)	0.393(157)	
$\langle g \rangle$	0.409(22)	0.411(87)	0.264(228)
$\langle g(I)/g(2_1^+) \rangle$ [a]		1.10(24)	0.79(69)

[a] $\langle g(I)/g(2_1^+) \rangle$ is the average of the $g(I)/g(2_1^+)$ obtained for the three runs.

The degree of alignment, $w(m=0)$, following the Coulomb excitation can be determined from the S^{meas} and the calculated P_i. Finally, the $\Delta\theta(2_1^+)$ can now be derived from S^{meas}, the known $S_i(\theta_0)$, P_i, $W_i(\theta_0)$, and ϵ^{meas} for the 2_1^+, 4_1^+, and 2_2^+ states. The results are summarized in Table IV.

The g factors are determined from the expression

$$\Delta\theta = g \frac{\mu_N}{\hbar} \int_{t_{\text{in}}}^{t_{\text{out}}} B(v(t),Z)\, e^{-t/\tau}\, dt, \tag{3}$$

where B is the transient field, τ the meanlife of the state being examined, and t_{in} and t_{out} are the mean entrance and exit times of the ions into or out of the ferromagnet.

The total cross sections for Coulomb excitation of the 2_1^+, 0_2^+, 2_2^+, 4_1^+, and 6_1^+ states under the experimental conditions of the experiment were calculated on the basis of the Winther–de Boer COULEX code (Table III). In practice, there exist many versions of the original code. The most significant difference between them concerns the selection of the *sign* of the electromagnetic matrix elements of the nuclear states. Several codes employ the convention $M(E\lambda) = -1^{\lambda} \cdot M_{\text{Winther-deBoer}}(E\lambda)$ and $M(M\lambda) = -1^{\lambda+1} \cdot M_{\text{Winther-deBoer}}(M\lambda)$. Often the sign of the matrix elements has no effect on the predicted populations. This situation pertains to the case of low excitation probabilities, when reorientation effects are negligible, or to the case in which the populated state can only be excited by one pathway. If these conditions do not apply, as is the case, for example, when the 2_1^+ state is excited either directly or in the decay of the 2_2^+ state, the interference between the different population pathways which arises from the choice of sign of the matrix element, needs to be taken into account. In the present experiment, the signs were chosen to fit the experimentally observed state populations.

The results of the analysis are presented in Table IV.

IV. DISCUSSION

The resulting ratio of g factors $g(4_1^+)/g(2_1^+) = 1.10(24)$ is in agreement with models of collective excitations, IBA models with either a restricted sd-boson or an extended sdg-boson basis [9], or models involving configuration mix-

ing [12]. Measurements of $g(2_1^+)$ of Nd, Sm, and Gd isotopes have supported the arguments for a subshell closure at $Z=64$ [4,10,11]. This subshell was assumed to vanish for $N=90$, an effect correlated with the onset of deformation. Does this description persist at higher angular momentum? Besides the measurement presented in this paper, there exists only one other measurement of $g(4_1^+)$ in the vibrational and transitional light nuclei of Nd, Sm, and Gd, and that is the measurement in ^{150}Sm [1,2]. Several conjectures have been advanced to explain the large ratio $g(4_1^+)/g(2_1^+)=1.60(12)$ observed in ^{150}Sm by Vass *et al.* [1].

(a) The 4_1^+ state is more deformed than the 2_1^+ state [12,13]. Can it be that the phase transition from spherical to deformed shape is more complete for the 4_1^+ state than for the 2_1^+ state? Calculations [15] show that the backbend is indeed sharper and occurs earlier for the 4_1^+ than for the 2_1^+ state. This explanation is supported by the observation that the ratio $B(E2;4_1^+\rightarrow 2_1^+)/B(E2;2_1^+\rightarrow 0_1^+)$ has a maximum for $N=88$ nuclei.

(b) Pairing is strong for neutrons but breaks down for protons at higher spins, a somewhat unlikely scenario [12]. In this case, as

$$g(2_1^+)\approx Z/A=0.41$$

and

$$g(4_1^+)\approx \frac{\mathcal{J}_{\pi,\mathrm{rigid}}}{\mathcal{J}_{\pi,\mathrm{rigid}}+\frac{2}{5}\mathcal{J}_{\nu,\mathrm{rigid}}}=\frac{Z}{Z+\frac{2}{5}N}=0.61,$$

$g(4_1^+)/g(2_1^+)=1.5$.

(c) The simplified model calculation in the Nilsson-Strutinsky + CBS approach [14] predicts that changes in the nuclear deformation and in pair fields occur with increasing spin for $N=88$ nuclei. However, the effect is small as confirmed by the recent measurement of the ratio $g(4_1^+)/g(2_1^+)\approx 1$ in ^{154}Dy [16,17].

(d) Configuration mixing plays a role. In the most naive shell model, it is possible to construct the low-lying states with $d_{5/2}$ protons and $h_{9/2}$ neutrons for which $g=1.13$ [12]. Thus, even a small admixture of such configurations could indeed result in magnetic moments that deviate from the predictions presented above. In fact, recent data on ^{146}Nd [18] show that the g factor of the 4_1^+ state is also markedly different from that of the 2_1^+ state.

It thus appears that ^{152}Gd, with $Z=64$ protons closing a magic subshell, may exhibit stronger collectivity than the neighboring nuclei with proton holes in the subshell. In these nuclei, single-particle effects can be enhanced. High precision systematics of g factors of the low excited states in nuclei with protons around the $Z=64$ subshell and neutron number above and below the $N=88$ boundary are necessary to assay the interplay between collective and single-particle configurations.

Experiments are underway in which the g factors of the low-lying excited states will be measured with significantly higher precision than available at present. These experiments involve Coulomb excitation, in inverse kinematics, of the states of interest in a beam of the relevant nuclei Nd, Sm, Gd, and Dy [8,18].

ACKNOWLEDGMENTS

The authors thank A. Lipski who has prepared the targets and Professor R. Casten and Dr. V. Zamfir for substantial discussions. We also are thankful to the accelerator staff of the Wright Nuclear Structure Laboratory for their support. This work was supported in part by the National Science Foundation.

[1] T. Vass, A.W. Mountford, G. Kumbartzki, N. Benczer-Koller, and R. Tanczyn, Phys. Rev. C **48**, 2640 (1993).
[2] A.P. Byrne, A.E. Stuchbery, H.H. Bolotin, C.E. Doran, and G.J. Lampard, Nucl. Phys. **A466**, 419 (1987).
[3] H. Armon, E.R. Bauminger, A. Diamant, I. Nowik, and S. Ofer, Nucl. Phys. **A233**, 385 (1974).
[4] N. Benczer-Koller, D.J. Ballon, and A. Pakou, Hyperfine Interact. **33**, 37 (1987).
[5] N.K.B. Shu, D. Melnik, J.M. Brennan, W. Semmler, and N. Benczer-Koller, Phys. Rev. C **21**, 1828 (1980).
[6] N. Benczer-Koller, M. Hass, and J. Sak, Annu. Rev. Nucl. Sci. **30**, 53 (1980).
[7] A. Piqué, J.M. Brennan, R. Darling, R. Tanczyn, D. Ballon, and N. Benczer-Koller, Nucl. Instrum. Methods Phys. Res. A **279**, 579 (1989).
[8] K.-H. Speidel, N. Benczer-Koller, G. Kumbartzki, C. Barton, A. Gelberg, J. Holden, G. Jakob, N. Matt, R.H. Mayer, M. Satteson, R. Tanczyn, and L. Weissman, Phys. Rev. C **57**, 2181 (1998).
[9] I. Morrison, Phys. Lett. B **175**, 1 (1986).
[10] N. Benczer-Koller, Y. Niv, M. Hass, D. Ballon, T. Bright, and S. Vajda, Ann. Isr. Phys. Soc. **7**, 133 (1984).
[11] A. Wolf, D.D. Warner, and N. Benczer-Koller, Phys. Lett. **158B**, 7 (1985).
[12] L. Zamick (private communication).
[13] R. Casten (private communication).
[14] R. Bengtsson and S. Åberg, Phys. Lett. B **172**, 277 (1986).
[15] J.Y. Zhang, Nucl. Phys. **A421**, 353c (1984).
[16] H. Hübel, S. Heppner, U. Birkental, G. Baldsiefen, A.P. Byrne, W. Schmidt, M. Bentley, P. Fallon, P.D. Forsyth, D. Howe, J.R. Roberts, H. Kluge, G. Goldring, A. Dewald, G. Siems, and E. Lubkiewicz, Prog. Part. Nucl. Phys. **28**, 295 (1992).
[17] U. Birkental, A.P. Byrne, S. Heppner, H. Hübel, W. Schmidt, P. Fallon, P.D. Forsyth, J.W. Roberts, H. Kluge, E. Lubkiewicz, and G. Goldring, Nucl. Phys. **A555**, 643 (1993).
[18] J. Holden, N. Benczer-Koller, G. Kumbartzki, T. Mertzimekis, K.-H. Speidel, I. Y. Lee, A. Macchiavelli, M. McMahan, L. Phair, and W. Rogers, Bull. Am. Phys. Soc. (to be published).